Interleukin-7-based identification of liver lymphatic endothelial cells reveals their unique structural features

Authors

Yilin Yang, Jain Jeong, Tingting Su, Sanchuan Lai, Pengpeng Zhang, Rolando Garcia-Milian, Morven Graham, Xinran Liu, Matthew J. McConnell, Teruo Utsumi, Joao Pereira, Yasuko Iwakiri

Correspondence

yasuko.iwakiri@yale.edu (Y. Iwakiri).

Graphical abstract

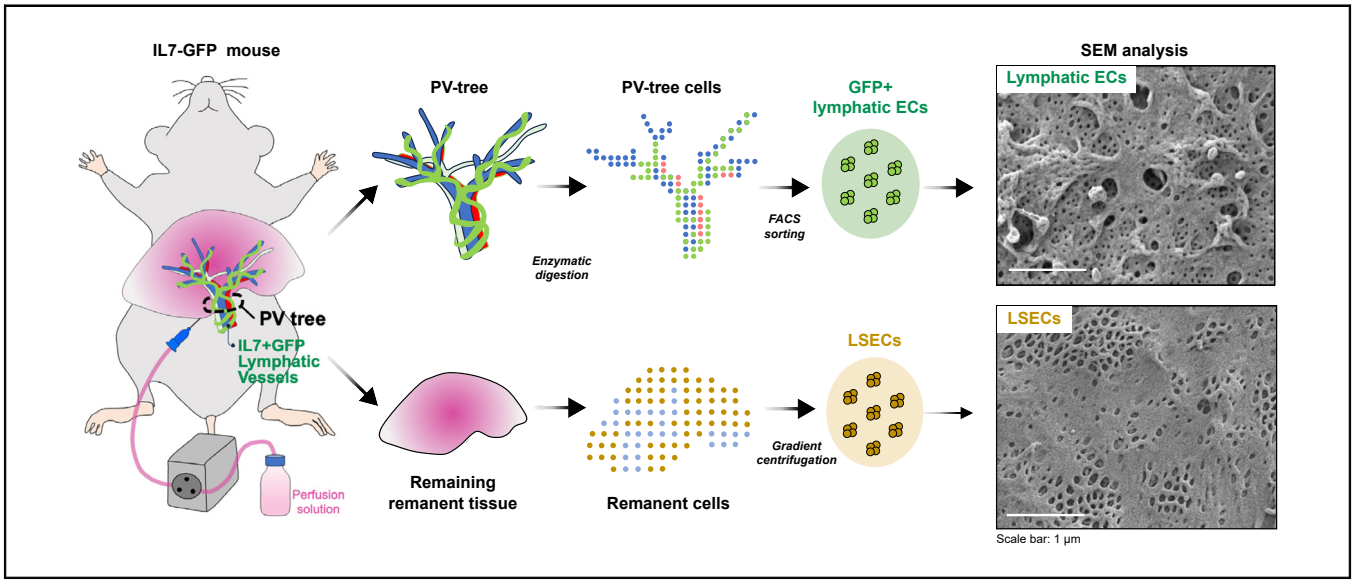

Highlights

- IL7 is a good marker of liver lymphatic endothelial cells (LyECs).
- We developed an isolation method for liver LyECs using IL7-GFP knockin mice.
- Our isolation protocol unveils the distinctive cell surface structure of LyECs.
- Novel genes affected in I/R-induced liver injury were identified in LyECs.

Impact and implications

Understanding the lymphatic system in the liver is challenging because of the absence of specific markers for liver LyEC. This study has identified IL7 as a reliable marker for LyECs, enabling the development of an effective method for their isolation, elucidating their unique cell surface structure, and identifying LyEC genes that undergo changes during liver damage. The development of IL7 antibodies for detecting it in human liver specimens will further advance our understanding of the liver lymphatic system in the future.

https://doi.org/10.1016/j.jhepr.2024.101069

Research article

JHEP|Reports

Interleukin-7-based identification of liver lymphatic endothelial cells reveals their unique structural features

Yilin Yang,[1] Jain Jeong,[1] Tingting Su,[1,2] Sanchuan Lai,[1,3] Pengpeng Zhang,[1,4] Rolando Garcia-Milian,[5] Morven Graham,[6] Xinran Liu,[6] Matthew J. McConnell,[1] Teruo Utsumi,[1] Joao Pereira,[7] Yasuko Iwakiri[1,*]

[1]*Department of Internal Medicine, Section of Digestive Diseases, Yale University School of Medicine, New Haven, CT, USA;* [2]*Department of Gastroenterology, First Affiliated Hospital, Zhejiang University School of Medicine, Hangzhou, China;* [3]*Department of Gastroenterology, Second Affiliated Hospital, Zhejiang University School of Medicine, Hangzhou, China;* [4]*The Transplantation Center of the Third Xiangya Hospital, Central South University, Changsha, China;* [5]*Bioinformatics Support Hub, Cushing/Whitney Medical Library, Yale University School of Medicine, New Haven, CT 06510, USA;* [6]*Center for Cellular and Molecular Imaging, Yale University School of Medicine, New Haven, CT, USA;* [7]*Department of Immunobiology and Yale Stem Cell Center, Yale University School of Medicine, New Haven, CT, USA*

JHEP Reports **2024.** https://doi.org/10.1016/j.jhepr.2024.101069

Background & Aims: The lymphatic system plays crucial roles in maintaining fluid balance and immune regulation. Studying the liver lymphatics has been considered challenging, as common lymphatic endothelial cell (LyEC) markers are expressed by other liver cells. Additionally, isolation of sufficient numbers of LyECs has been challenging because of their extremely low abundance (<0.01% of entire liver cell population) in a normal liver.
Methods: Potential LyEC markers was identified using our published single-cell RNA sequencing (scRNA-seq) dataset (GSE147581) in mouse livers. Interleukin-7 (IL7) promoter-driven green fluorescent protein knock-in heterozygous mice were used for the validation of IL7 expression in LyECs in the liver, for the development of liver LyEC isolation protocol, and generating liver ischemia/reperfusion (I/R) injury. Scanning electron microscopy was used for the structural analysis of LyECs. Changes in LyEC phenotypes in livers of mice with I/R were determined by RNA-seq analysis.
Results: Through scRNA-seq analysis, we have identified IL7 as an exclusive marker for liver LyECs, with no overlap with other liver cell types. Based on IL7 expression in liver LyECs, we have established an LyEC isolation method and observed distinct cell surface structures of LyECs with fenestrae and cellular pores (ranging from 100 to 400 nm in diameter). Furthermore, we identified LyEC genes that undergo alterations during I/R liver injuries.
Conclusions: This study not only identified IL7 as an exclusively expressed gene in liver LyECs, but also enhanced our understanding of LyEC structures and demonstrated transcriptomic changes in injured livers.
Impact and implications: Understanding the lymphatic system in the liver is challenging because of the absence of specific markers for liver LyEC. This study has identified IL7 as a reliable marker for LyECs, enabling the development of an effective method for their isolation, elucidating their unique cell surface structure, and identifying LyEC genes that undergo changes during liver damage. The development of IL7 antibodies for detecting it in human liver specimens will further advance our understanding of the liver lymphatic system in the future.

Introduction

The lymphatic vascular system plays active roles in maintaining fluid balance, immune regulation and tumour growth.[1,2] In the liver, increased lymphatic vessel expansion, particularly in the portal tract area, is observed in various pathological conditions. However, the mechanistic studies on how the liver lymphatic system is involved in the development of disease is limited. This is because investigating lymphatic endothelial cells (LyECs) and lymphatic functions is thought to be challenging, as typical LyEC markers are expressed by other liver cells.[3–7] In addition, given that LyECs account for the smallest population among all endothelial cell (EC) populations in the mouse liver (<1%), obtaining enough LyECs is challenging.[8] Thus, the aim of this study is to identify a unique gene that is expressed in LyECs, but not in other major liver cells, and to apply this knowledge for isolation and characterization of LyECs in normal and diseased livers.

General LyEC markers in most tissues and organs include lymphatic vessel endothelial hyaluronan receptor 1 (LYVE1),[9,10] vascular endothelial growth factor receptor 3 (VEGFR3, also known as Flt4),[11] podoplanin (PDPN),[12] and prospero homeobox

Keywords: Lymphatic endothelial cell; IL7; Ischemia/reperfusion; Liver lymphatic system; Isolation method; Liver injury; Transcriptomics; Liver sinusoidal endothelial cell; Hepatic lymphatic system; scRNA-seq.
Received 19 November 2023; received in revised form 1 March 2024; accepted 11 March 2024; available online 18 March 2024
* Corresponding author. Address: Section of Digestive Diseases, Department of Internal Medicine, Yale University School of Medicine, TAC S223B, 333 Cedar Street, New Haven, CT 06520, USA. Tel.: +1-203-785-6204; Fax: +1-203-785-7273.
E-mail address: yasuko.iwakiri@yale.edu (Y. Iwakiri).

protein 1 (PROX1).[13] In the liver, however, hepatocytes express PROX1, and liver sinusoidal endothelial cells (LSECs, major liver ECs) express both VEGFR3 and LYVE1. Although PDPN may be the most frequently used LyEC marker for immunolabeling, it is expressed by cholangiocytes and myofibroblasts as well as mesothelial cells in liver capsules. Accordingly, expression of these common LyEC markers in other liver cells make it difficult to study detailed molecular mechanisms of lymphatic vessel (LV) functions in a LyEC-specific manner in the liver. Therefore, the identification of novel LyEC markers in the liver is an urgent need and will significantly advance our understanding of the liver lymphatic system.

We recently identified six heterogeneous liver EC clusters using single-cell RNA sequencing (scRNA-seq) analysis of the mouse liver EC population.[8] One of them was the LyEC cluster based on the expression of *Lyve1*, *Flt4*, *Pdpn*, and *Prox1*. The analysis also identified several unique genes that were highly expressed in LyECs. However, since the scRNA-seq analysis was conducted only on the liver EC population, excluding other liver cells, we did not know whether these unique genes could be expressed exclusively in LyECs or also expressed in other liver cell types. Recent scRNA-seq analysis on human liver non-parenchymal cells has also identified heterogeneous liver EC clusters, including the LyEC cluster.[14] However, there has been no cross-species comparison of human and mouse LyEC expression profiles, nor has there been verification of unique gene markers.

In this study, we have identified interleukin-7 (IL7) as a useful LyEC marker in the liver, minimally or not expressed by other liver cell types. IL7 is a cytokine that plays a critical role in the development and maintenance of T lymphocytes, B lymphocytes, and innate lymphoid cells.[15] Because anti-IL7 antibodies have failed to reliably identify IL7^{+} cells in tissue sections of wild-type and IL7-deficient mice, multiple IL7 reporter mice have been generated.[16] Studies utilizing IL7-green fluorescent protein (GFP) reporter mice (*IL7*$^{GFP/+}$ knock-in mice) showed strong IL7 expression in LyECs of the lymph node medulla, skin epidermis, lung, and intestinal tissues,[17,18] which are in line with our finding of IL7 expression in liver LyECs. Further, utilizing the portal tree (a.k.a. biliary tree) where most of LVs are located and *IL7*$^{GFP/+}$ knock-in mice, we have established an efficient isolation protocol for liver LyECs along with LSEC isolation from the same animals.

With this isolation protocol, we have also identified a unique cell membrane structure of LyECs distinct from that of LSECs. In addition to the fenestrae structure typical of LSECs, LyECs showed larger pores (~500 nm) with filopodium-like membrane protrusion on their membrane surface. This protocol also allowed us to identify transcriptomic changes and related functional changes of LyECs caused by ischemia/reperfusion (I/R)-induced liver injury.

Materials and methods

Detailed materials and methods can be found in the Supplementary material.

Animal experiments

To examine changes of LyECs as a result of liver I/R injury, we used IL7 promoter-driven GFP knock-in heterozygous mice (*IL7*$^{GFP/+}$ knock-in mice, a kind gift from Dr Joao Pereira, Yale University)[18] at the age of approximately 2 months. For a liver I/R model, a small clamp was placed on the portal vein and bile duct at the root of three major liver lobes to cause a 70% hepatic ischemia, followed by its removal in 60 min, resupplying blood and oxygen to the ischemic liver lobes. The liver and blood were collected 3 days after the surgery. All animal experiments were approved by the Institutional Animal Care and Use Committee of the Veterans Affairs Connecticut Healthcare System (#YI0001) and performed in adherence with the National Institutes of Health Guidelines for the Use of Laboratory Animals.

Single-cell RNA sequencing analysis

All analyses were performed in the Seurat R package (version 4.3.0). For mouse liver scRNA-seq analysis, we reassessed our previously published data[8,14] on non-apoptotic ECs isolated from livers of control or fibrotic EC-specific GFP reporter mice (Cdh5-Cre-mTmG$^{+/+}$ mice). Genes expressed in less than three cells and cells that expressed <200 genes, >8,000 genes, or mitochondrial gene contents over 40% of the total unique molecular identifier (UMI) count were excluded. Uniform Manifold Approximation and Projection (UMAP) was used to visualize cell clusters after normalizing and scaling the data with one to 20 principal components, and cell clusters were identified and divided into subsets for analysis in Fig. 1.

For human liver scRNA-seq analysis, a previously published human scRNA-seq dataset[14] was downloaded from Gene Expression Omnibus (GEO) under an accession number GSE136103. The scRNA-seq results from five healthy human livers in the original dataset was used. Genes expressed in fewer than three cells were excluded, as well as cells that expressed <300 genes, >6,000 genes, or mitochondrial gene contents >30% of the total UMI count. After normalizing and scaling the data, we used UMAP to visualize cell clusters with one to 40 principal components. Cells clusters were annotated according to the original study.

Primary mouse liver cell isolation

Refer to the Supplementary data.

Primary human cells

Refer to the Supplementary data.

Quantitative real-time polymerase chain reaction

Refer to the Supplementary data.

Scanning electron microscopy

Refer to the Supplementary data.

Immunofluorescence

Refer to the Supplementary data.

3D immunofluorescence imaging

Refer to the Supplementary data and the publication by Jeong *et al.*[19]

RNA sequencing analysis of isolated liver LyECs

Refer to the Supplementary data.

Flow cytometry

Refer to the Supplementary data.

Statistical analysis

Data were expressed as mean ± standard error of mean (SEM). Statistical analysis was performed using the GraphPad Prism version 8.0 (GraphPad Software, San Diego, CA). Statistical

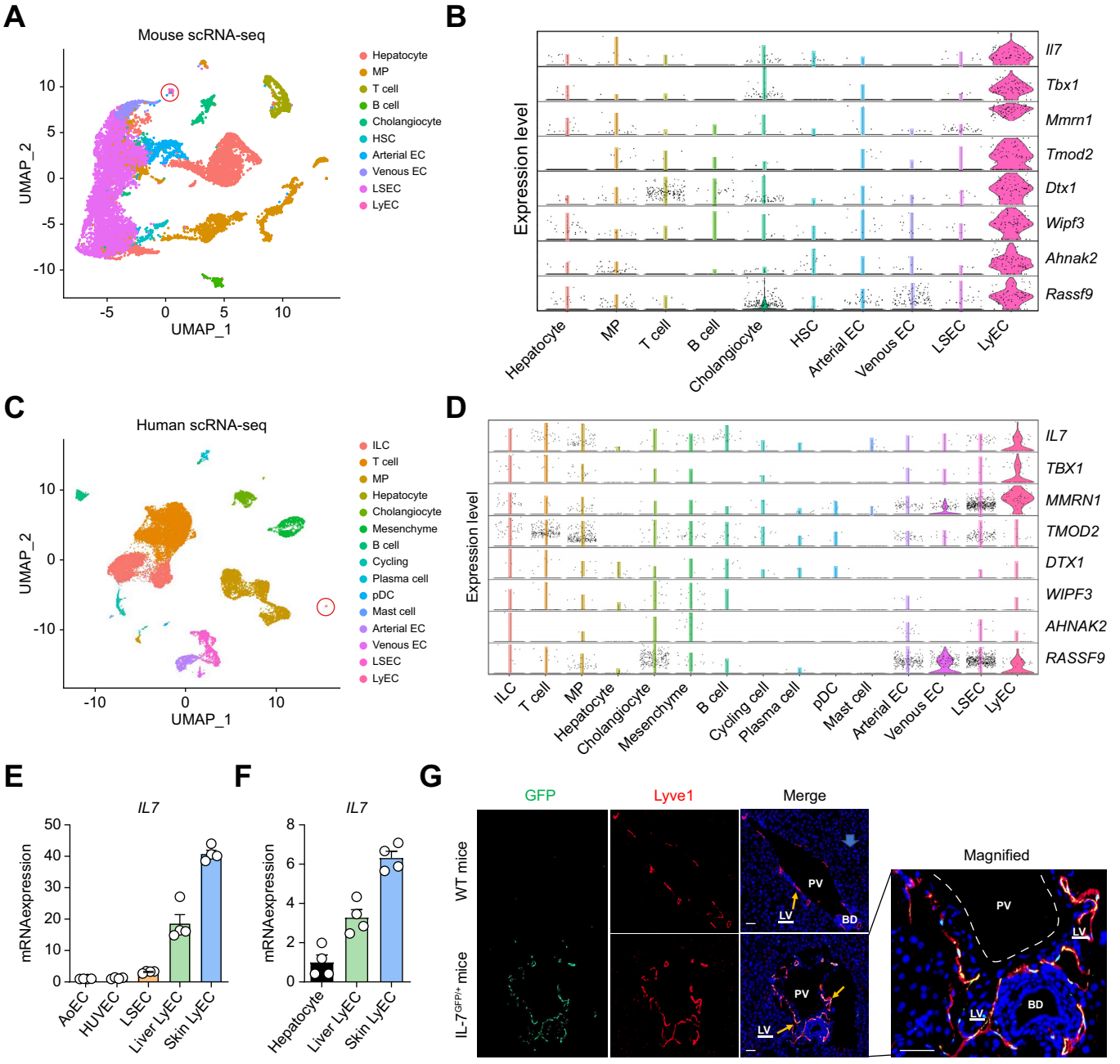

Fig. 1. IL7 is highly expressed in liver lymphatic endothelial cells. (A) Uniform Manifold Approximation and Projection (UMAP) showing clusters of liver cells from healthy (n = 3) and cirrhotic (n = 3) mouse livers (Cdh5-Cre-mTmG$^{+/+}$ mice) (GSE147581). The identified 10 liver cell clusters were defined by marker genes as hepatocyte, MP (macrophage), T cell, B cell, cholangiocyte, HSC (hepatic stellate cell), arterial EC (arterial-like EC), venous EC (central venous EC), LSEC (liver sinusoidal EC), and LyEC (lymphatic EC). Each dot represents a single cell. The LyEC cluster is marked with a red circle. (B) Violin plots of gene expression of *Il7*, *Tbx1*, *Mmrn1*, *Tmod2*, *Dtx1*, *Wipf3*, *Ahnak2*, and *Rassf9* in mouse liver cells. (C) UMAP showing clusters of liver cells from healthy human livers (n = 5) (GSE136103). The identified 15 liver cell clusters were defined by marker genes as ILC (innate lymphoid cell), T cell, MP (mononuclear phagocyte), hepatocyte, cholangiocyte, mesenchyme (mesenchyme cell), B cell, cycling cell, plasma cell, pDC (plasmacytoid dendritic cell), mast cell, arterial EC, venous EC, LSEC, and LyEC. Each dot represents a single cell. The LyEC cluster is marked with a red circle. (D) Violin plots of gene expression of *IL7*, *TBX1*, *MMRN1*, *TMOD2*, *DTX1*, *WIPF3*, *AHNAK2*, and *RASSF9* in human liver cells. (E) mRNA expression levels of IL7 in primary human aortic ECs (AoECs), primary human umbilical veinous ECs (HUVECs), primary human LSECs, primary human hepatic lymphatic ECs (Liver LyECs), and primary human dermal lymphatic ECs (Skin LyECs) (n = 4). Data are the mean ± SEM. (F) mRNA expression levels of IL7 in primary human hepatocytes, primary human liver LyECs, and primary human skin LyECs (n = 4). (G) Green fluorescent protein (green: IL7-GFP) and Lyve1 (red: a marker of lymphatic vessels) immunolabeling in the livers of WT and *IL7*$^{GFP/+}$ knock-in mice. DAPI (blue: nuclei). BD, bile duct; LV, lymphatic vessel; PV, portal vein (n = 5). Scale bar: 50 μm. Data are the mean ± SEM.

significance was determined by unpaired *t* test for comparisons of two groups or one-way ANOVA followed by Tukey's test for comparisons of multiple groups. A *p* value of <0.05 was considered as statistically significant.

Results

IL7 is a marker of liver lymphatic endothelial cells

We explored specific markers of liver lymphatic ECs, utilizing the 10 × scRNA-seq data in our previous study on an EC-enriched liver cell population isolated from healthy and cirrhotic livers of EC-specific GFP reporter mice (Cdh5-Cre-mTmG$^{+/+}$ mice).[8] Cirrhosis in these mice was induced by inhalation of carbon tetrachloride for 3 months. Our reanalysis revealed 19 cell clusters from 13,969 cells with their respective marker genes (Fig. S1A and B). We then consolidated them into 10 clusters of liver cell populations based on marker genes described in our previous study,[8] which included hepatocytes, macrophages (MP), T cells, B cells, cholangiocytes, hepatic stellate cells (HSCs), arterial ECs, venous ECs, LSECs, and LyECs (Fig. S1A and C). The LyEC cluster was identified (Cluster 18 in Fig. S1A and B) based on the expression of three well-known LyEC markers, Lyve1, Pdpn, and Prox1(Fig. S1C). From a list of genes uniquely expressed in the LyEC cluster (Table S1), we selected eight genes from the top 20, namely *Il7, Tbx1, Mmrn1, Tmod2, Dtx1, Wipf3, Ahnak2*, and *Rassf9*, for further verification (Fig. 1B). These genes were selected because their expression was not detected in other liver ECs, such as arterial ECs, venous ECs, and LSECs.

For a cross-species verification, we also reanalyzed a scRNA-seq data on non-parenchymal cells of healthy human livers published by Ramachandran *et al.*[14] and assembled 31 cell clusters from 35,067 cells with their respective gene markers (Fig. S2A and B). We further grouped them into 15 clusters according to marker genes used in their study and annotated them as innate lymphoid cell (ILC), T cell, mononuclear phagocytes (MP), hepatocyte, cholangiocyte, mesenchyme, B cell, cycling cell, plasma cell, plasmacytoid dendritic cell (pDC), mast cell, arterial EC, venous EC, LSEC, and LyEC (Fig. 1C and Fig. S2C). The LyEC cluster was identified to be Cluster 29 (Fig. S2A and B) based expression of *CCL21*, *PDPN*, and *PROX1* (Fig. S2C). We then examined whether the eight LyEC marker genes selected from our mouse scRNA-seq data were expressed specifically in the human LyEC cluster and found *IL7, TBX1*, and *MMRN1* specifically expressed by human liver LyECs as well with the other genes showing no specific or low expression (Fig. 1D).

We also examined whether our selected eight LyEC genes could be specific to liver LyECs by screening their expression in primary human aortic ECs (AoECs), primary human umbilical venous ECs (HUVECs), primary human LSECs, primary human skin LyECs, and primary human liver LyECs. The identity of these ECs was confirmed by expression of *DLL4* (an arterial EC marker), *EPHB4* (a venous EC marker), *PROX1* and *PDPN* (LyEC markers). LSEC identity was validated by expression of *FLT4* in the absence of expression of *PROX1* and *PDPN* (Fig. S3A). Expression levels of the eight LyEC genes in these ECs were presented in Fig. 1E and Fig. S3B, showing specific gene expression of IL7 in both primary human liver and skin LyECs with the other genes not exhibiting such LyEC specificity.

IL7 was reported to be expressed in hepatocytes and to play a role in the survival of naive and memory T cells.[20] However, the identity and distribution of IL7-expressing cells in the liver in physiological conditions have still been unclear because of its very low mRNA and protein levels, making its detection difficult. We compared IL7 mRNA levels between primary human hepatocytes and primary human liver or skin LyECs and found significantly higher IL7 expression in LyECs and minimal expression in hepatocytes (Fig. 1F). IL7 gene expression was also minimal in human cholangiocytes and hepatic stellate cells (Fig. S4A). Further, immunofluorescence staining of livers from *IL7*$^{GFP/+}$ knock-in mice showed colocalization of GFP and Lyve1 (a LyEC marker) in the portal area, confirming that a majority of GFP-positive cells (IL7-expressing cells) are LyECs with no measurable detection of *Il7*-driven GFP in hepatocytes (Fig. 1G).

To evaluate IL7 levels in the mouse liver at a whole organ level, we compared whole-tissue IL7 and GFP mRNA expression levels between the liver and the thymus, a lymphoid organ known to produce abundant IL7.[21] We observed that liver tissue IL7 gene expression was very low compared to that of the thymus, which was consistent with GFP mRNA levels in these two organs (Fig. S4C and D). Collectively, these observations show that IL7 is expressed in LyECs, but not in other liver cell types, and can thus serve as an excellent marker of liver LyECs. *Il7*$^{GFP/+}$ knock-in mice, which had been used to mark LyEC in the lung and lymph nodes,[18] show GFP expression specifically in liver LyECs as well, so these mice can be used to label liver lymphatics.

IL7-expressing GFP+ cells isolated from the liver portal venous biliary tree cell fraction are liver LyECs

Lack of specific LyEC markers has been one of the hurdles for efficient isolation of liver LyECs[3] on top of their very small portion of the liver EC population in the normal liver.[8,22] As liver lymphatic vessels are predominantly located in the portal area, we hypothesized that isolating LyECs from the liver portal venous biliary tree (PV tree) fraction could enhance their yield and isolation efficiency. To test this hypothesis, we established a protocol to isolate IL7-expressing GFP+ cells from PV tree cell fractions of *IL7*$^{GFP/+}$ knock-in mice (Fig. 2A). Liver collagenase perfusion separated the PV tree fraction that included bile ducts, portal vein, hepatic artery, and lymphatic vessels from the parenchymal and non-parenchymal fractions. Whole-mount 3D immunofluorescence imaging of these PV trees isolated from *IL7*$^{GFP/+}$ knock-in mice demonstrated enriched GFP and Lyve1 positive lymphatic vessels (Fig. 2B). As a positive control, Fig. S5 presents 3D images of mesenteric lymphatic vessels, which similarly show GFP and Lyve1 positive lymphatic vessels. We then further digested the PV tree to isolate its constituent cells (Fig. 2A) and compared them with components of the liver parenchymal cell or non-parenchymal cell fraction. The liver parenchymal cell fraction mostly contained hepatocytes, while the non-parenchymal fraction included LSECs, Kupffer cells, and hepatic stellate cells, and could be used to isolate LSECs. qPCR analysis of liver cell fractions (parenchymal cells, non-parenchymal cells, and PV tree cells) detected highest expression of IL7 and GFP in the PV tree cell fraction, as well as highest expression of *Ccl21a* and *Pdpn* (LyEC markers) (Fig. 2C), suggesting the congruence between IL7-expressing cells and LyECs. We also examined the GFP+ cell frequency in parenchymal, non-parenchymal, and PV tree cell suspensions by flow cytometry, and found that GFP+ cells were almost absent from the

parenchymal cell fraction, slight in the non-parenchymal cell fraction (∼0.07%), and highest in the PV tree cell fraction(∼1%) (Fig. 2D). All these observations indicate that the PV tree cell fraction contains highest IL7-expressing GFP+ cells in the livers of *IL7*$^{GFP/+}$ knock-in mice.

To confirm the identity of GFP+ cells in liver PV tree cell fractions from *IL7*$^{GFP/+}$ knock-in mice, we examined expression of Pdpn and CD31 in GFP+ cells. Flow cytometry analysis of gated GFP+ cells showed a ∼89% purity of LyECs (Pdpn+ CD31+) (Fig. 2E). In accordance with the flow cytometry analysis, immunofluorescence staining of fluorescence-activated cell sorting (FACS) sorted GFP+ cells from the PV tree cell fraction showed ∼90% GFP+ Pdpn+ CD31+ population (Fig. 2F), indicating that GFP+ cells from the PV tree cell fraction are LyECs. We have thus established a simple and efficient isolation method for liver LyECs using *IL7*$^{GFP/+}$ knock-in mice.

Morphological features of liver LyECs *vs.* LSECs isolated from *IL7*$^{GFP/+}$ knock-in mouse

An additional advantage of our isolation method is to achieve isolation of both liver LyECs and LSECs from the same *IL7*$^{GFP/+}$ knock-in mouse (Fig. 2A). This allowed us to compare their morphological differences by scanning electron microscopy (SEM) for the first time (Fig. 3A and B). LSECs represent the major EC population in the liver and their morphology has been characterized in many studies,[23,24] thus serving as a reference for this comparison. Fig. 3A compares an SEM image of liver LyECs with that of LSECs collected from the same mouse 4 h after seeding on fibronectin-coated plates. Like LSECs, liver LyECs presented sieve-structure on their surface. However, cellular pores on liver LyECs were larger in diameter (100–400 nm) and greater in variation than those of LSECs (100–200 nm in diameter). We also took SEM images of liver LyECs and LSECs cultured for 16 h after seeding (Fig. 3B) and observed loss of the surface sieve-structure on both cell types more dramatically in LyECs with decreased cellular pore diameters to 40–100 nm in LyECs and 60–150 nm in LSECs after long-term *in vitro* culture.

I/R injury alters transcriptomic profiles in liver LyECs

A recent study reported that hepatic I/R injury enhanced liver lymphangiogenesis with the lymphatic vessel area and density increasing in 24 h after I/R surgery and culminating at 72 h.[25] However, it was not known whether I/R injury could change LyEC characteristics. We leveraged our liver LyEC isolation method to examine liver LyEC biology in a mouse model of I/R. We first evaluated lymphatic vessels in the livers of *IL7*$^{GFP/+}$ knock-in mice subjected to sham or 3-day I/R (3d-I/R) surgery and observed increased GFP-positive cells co-localized with Lyve1 in the livers of 3d-I/R mice (Fig. 4A and B), indicating that IL7 remains expressed exclusively in LyECs under liver I/R injury. Increased IL7 mRNA levels were also detected in liver tissue from 3d-I/R mice (Fig. 4C) with their positive correlation with hepatic LV numbers (Fig. 4D). Consistently, GFP expression was also significantly increased in liver tissue from 3d-I/R mice and was positively correlated with hepatic LV numbers (Fig. S6A and B). These results further support IL7 as a reliable marker of hepatic LyECs even during pathological conditions such as liver I/R injury.

To further understand the biology of liver LyECs in I/R injury, we isolated hepatic LyECs (GFP^{+} cells) from *IL7*$^{GFP/+}$ knock-in mice with sham or 3d-I/R surgery by FACS and performed RNA-seq analysis. We detected a significantly increased number of GFP+ cells in the liver PV tree cell fractions isolated from 3d-I/R mice than those from sham mice (∼1.8-fold change, Fig. S6C), consistent with increased lymphangiogenesis in the 3d-I/R group shown in Fig. 4A and B.

A volcano plot shows a comprehensive gene profile from the RNA-seq analysis, in which red and green dots represent upregulated and downregulated genes, respectively (Fig. 4E). We identified 46 differentially expressed genes (DEGs) between the 3d-I/R and sham groups with 38 genes upregulated and eight genes downregulated in the 3d-I/R group. A heatmap of the 46 DEGs is presented in Fig. 4F. Gene set enrichment analysis (GSEA) revealed that I/R injury could activate vasculature-related pathways such as extracellular matrix (ECM)-related pathways, endothelial cell proliferation, and leukocyte adhesion to vascular endothelial cells and suppress inflammatory responses (Fig. 4G).

Discussion

This study identified IL7 as a useful LyEC marker in the liver and established a protocol for isolation of LyECs from the portal tree fraction of the liver of *IL7*$^{GFP/+}$ knock-in mice. Importantly, a unique LyEC cell surface structure is revealed using our isolation protocol. Further, we identified novel genes in LyECs that are altered in I/R-induced liver injury.

In the liver, LSECs share similar phenotypes to LyECs. They both have minimal basement membranes with loosely organized cell junctions. LSECs express some LyEC markers, such as Lyve1, VEGFR3(Flt4), and CLEC4M (a C-type lectin receptor, also known as LSIGN, CD209L, or CD299).[26,27] In addition, both LSECs and LyECs have immunological functions and are able to influence the composition of hepatic immune populations.[28] However, the role of liver LyECs has often been overlooked compared with that of LSECs. Thus, our identification of IL7 as a specific marker of hepatic LyECs is a crucial advancement and will significantly contribute to the study of the hepatic lymphatic system.

Isolation of LyECs is challenging because they constitute only a small fraction of the total liver cell population. LSECs are the major ECs in the liver, accounting for nearly 90% of all the liver EC population, whereas LyECs occupy only ∼0.12% of the liver EC population.[8] Therefore, their efficient isolation is particularly important. An isolation protocol recently reported for liver LyECs showed around 2,200 LyECs isolated from the non-parenchymal cell fraction per naive mouse liver.[22] To improve the isolation efficiency of LyECs, we utilized the portal tree fraction of the liver and *IL7*$^{GFP/+}$ knock-in mice to enrich and specifically mark liver LyECs. As a result, we achieved isolation of 20,000∼40,000 LyECs per mouse liver.

To our knowledge, the cellular architecture of LyECs remains largely unknown. Our study showed that the surfaces of both LSECs and LyECs displayed a sieve-like structure called opened fenestrae (usually 100–200 nm), which form a permeable barrier allowing direct communication between hepatocytes and the bloodstream. The LyEC surface, however, revealed more heterogeneous sieve-like structures and pores (100–400 nm) with

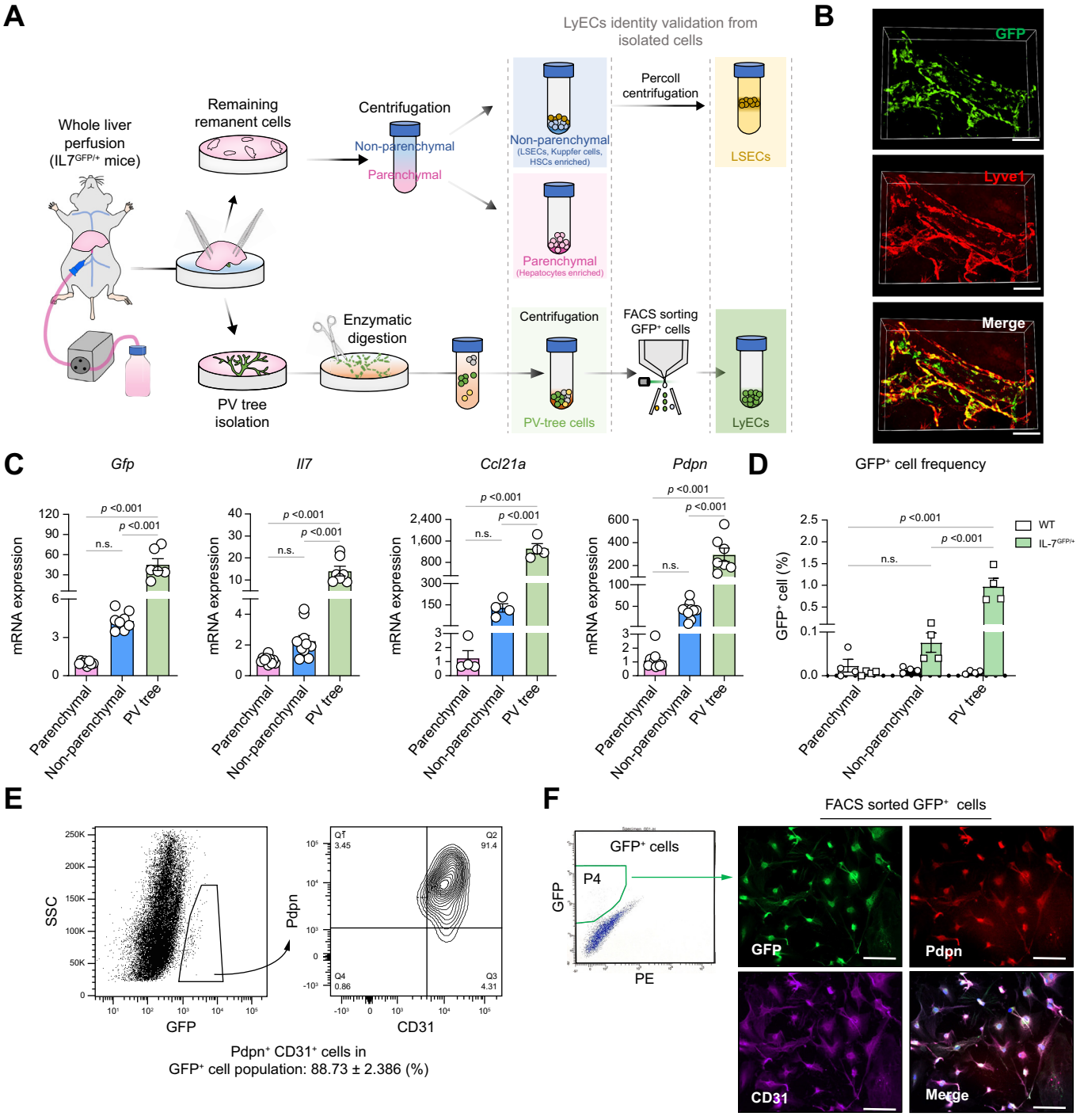

Fig. 2. Lymphatic EC isolation from the portal venous biliary tree cell fraction of *IL7*$^{GFP/+}$ knock-in mouse liver. (A) Cell isolation workflow using *IL7*$^{GFP/+}$ knock-in mice. After liver collagenase perfusion, liver cells were separated into digested cell suspension and the remaining residual with biliary tree structure (PV tree). The digested cell suspension was centrifuged to separate parenchymal and non-parenchymal cell fractions (in the pink and blue backgrounds, respectively). The non-parenchymal cell fraction was used for isolation of liver sinusoidal ECs (LSECs) by Percoll centrifugation. The undigested PV tree was used for immunofluorescence imaging or further digested to obtain a PV tree cell faction (in the green background). The PV tree cell faction was further sorted by FACS to isolate GFP+ LyECs. (B) Whole-mount 3D immunofluorescence images of GFP (green: IL7-GFP) and Lyve1 (red: a marker of lymphatic vessels) in PV trees from *IL7*$^{GFP/+}$ knock-in mice. Scale bar: 100 μm. (C) Expression levels of GFP, IL7, and lymphatic markers (Ccl21a and Pdpn) in parenchymal/non-parenchymal/PV tree cell fractions (n = 7). Data are the mean ± SEM. One-way ANOVA with Tukey's multiple comparison test. (D) GFP+ cell frequency was quantified based on the gated GFP+ subset (n = 4). Data are the mean ± SEM. One-way ANOVA with Tukey's multiple comparison test. (E) Parenchymal/non-parenchymal/PV tree cell fractions were stained with anti-Pdpn and anti-CD31 antibodies. The left panel shows gated GFP+ cells in the liver PV tree cell fractions of *IL7*$^{GFP/+}$ knock-in mice, and the right panel shows the percentages of Pdpn+ CD31+ cells in gated GFP+ cells (n = 3). Given their low percentages, enough GFP+ cells could not be isolated from the

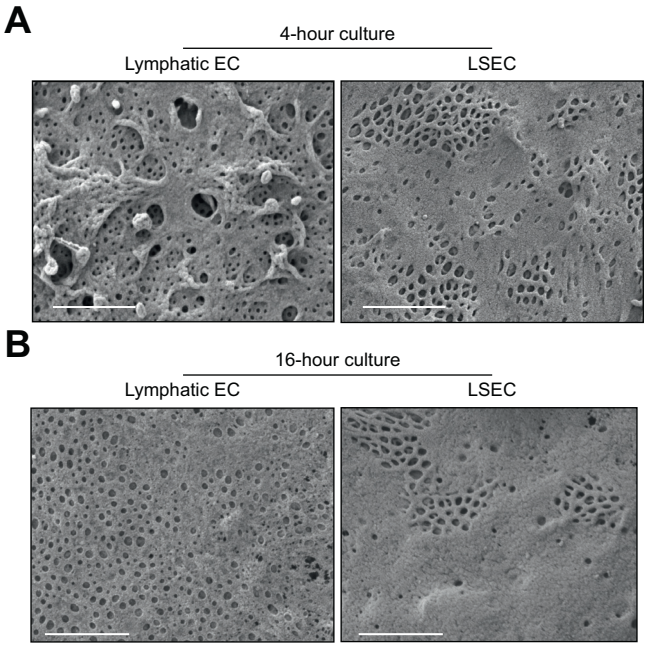

Fig. 3. Morphological characterization of LyECs and LSECs isolated from same *IL7*$^{GFP/+}$ knock-in mice. (A,B) Liver lymphatic endothelial cells (LyECs) and liver sinusoidal endothelial cells (LSECs) were isolated from same *IL7*$^{GFP/+}$ knock-in mice and seeded on fibronectin-coated plates. (A) Scanning electron microscopy images of liver LyECs and LSECs cultured for 4 h and 16 h (B) after isolation. Scale bar: 1 μm.

protruding objects. Similar to LSECs, longer cell culture (*e.g.* 16 h) dramatically diminished these unique structures. We speculate that large pores, not fenestrae structure, in LyECs may allow immune cells to easily move from the outer side of the lymphatic vessels (*e.g.* the space of Mall) into its lumen side and help their discharge. It is also possible that loss of pore structure in the cell surface may occur in pathological conditions and decrease efficiency of lymphatic drainage, resulting in prolonged inflammation in the liver. Further studies are important to elucidate what makes LyEC surface structure different from that of LSECs and to determine whether the pore structure of LyECs is maintained or lost in the pathogenesis of liver disease.

There is a potential that varying isolation procedures between the non-parenchymal cell fraction and the PV trees may result in differences in cell surface structures between LSEC and LyECs. However, we think it is unlikely, as the distinctive structural features (large pore and protrusion) were significant lost 16 h after LyECs were plated. If these unique features were a result of additional stress or a different isolation procedure applied to the PV tree, they would not have disappeared within the 16-h period after plating.

Hepatic lymphatics participate in the clearance of dead tissues and contribute to the reparative process after acute hepatic injury. However, it remains largely unknown whether functional changes of LyECs accompany liver repair. A recent study using a mouse model of hepatic I/R injury showed enhanced lymphangiogenesis around the portal tract with increased expression of pro-lymphangiogenic growth factors such as vascular endothelial growth factor (VEGF)-C and VEGF-D.[25] Activation of VEGFR3 signaling improved liver repair by promoting lymphangiogenesis and regulating the number of reparative macrophages.[25] Consistent with their observation, we found increased numbers of liver LVs in a hepatic I/R injury model using *IL7*$^{GFP/+}$ knock-in mice. In addition, our RNA-seq data on isolated LyECs from sham or I/R livers from *IL7*$^{GFP/+}$ knock-in mice revealed an upregulated EC proliferation pathway, upregulated leukocyte adhesion to ECs, upregulated ECM-related pathways, and downregulated inflammatory response in LyECs in response to I/R injury, suggesting functional changes of LyECs and the role of LyECs in tissue remodelling after hepatic injury.

It has been thought that hepatocytes are the major sources of IL7 in the liver.[20,29–31] However, these studies did not examine IL7 expression in hepatic LyECs or lymphatic vessels. In our study, IL7 expression in hepatocytes was very minimal in the normal postnatal liver, whereas LyECs expressed IL7 seven times more highly than hepatocytes. Our immunofluorescence staining of normal liver tissue from *IL7*$^{GFP/+}$ knock-in mice also showed a strong GFP signal mostly in LyECs, not in hepatocytes, indicating LyECs are the major sources of IL7 in the liver. GFP staining in the livers of *IL7*$^{GFP/+}$ knock-in mice with sham or I/R surgery also showed no induction of hepatocyte-derived IL7, suggesting that IL7 can still serve as a good marker of LyECs in I/R injury. However, it is interesting to note that hepatocytes started to express IL7 in cell culture conditions in a time-dependent manner, whereas freshly isolated hepatocytes without attaching to culture dishes showed minimal or no IL7 expression. This may indicate that caution would be needed regarding IL7 levels in cultured hepatocytes and that a long-term cell culture condition could cause overestimation of IL7 levels in hepatocytes.

Studies have shown that IL7 is produced by LyECs in the skin,[17,32] lymph node,[17] and lung.[18] Furthermore, it was demonstrated that IL7 induces lymphangiogenesis in cultured skin LyECs, promotes fluid uptake by lymphatic capillaries, and enhances lymphatic drainage in ear skin.[32] Thus, IL7 may also play a crucial role in maintaining LyECs integrity and their function in the liver. This topic is essential for future exploration and will contribute to advancing our understanding of the regulation of lymphatic function in both normal and diseased liver.

To the best of our knowledge, there is currently no well-established IL7 antibody available, thereby limiting the application of IL7 for immunolabeling to detect lymphatic vessels in human livers or for isolating LyECs in human livers. The development of such antibody is essential to advance our understanding of lymphatic systems in human livers. Alternatively, the validation of our findings can be achieved through *in situ* hybridization of IL7 RNA in human liver biopsies.

In conclusion, the identification of IL7 as an excellent marker for liver LyECs, together with the establishment of isolation of LyECs from the portal tree fraction, will advance the study of the hepatic lymphatic system. Mechanistic implications of the

parenchymal and non-parenchymal cell fractions. (F) Immunolabeling of GFP, Pdpn, and CD31 in FACS isolated GFP+ cells in liver PV tree cell fractions of *IL7*$^{GFP/+}$ knock-in mice (n = 3). Scale bar: 1 μm. EC, endothelial cell; FACS, fluorescence-activated cell sorting; GFP, green fluorescent protein; IL7, interleukin 7; LyECs, lymphatic endothelial cells; Lyve1, hyaluronan receptor 1.

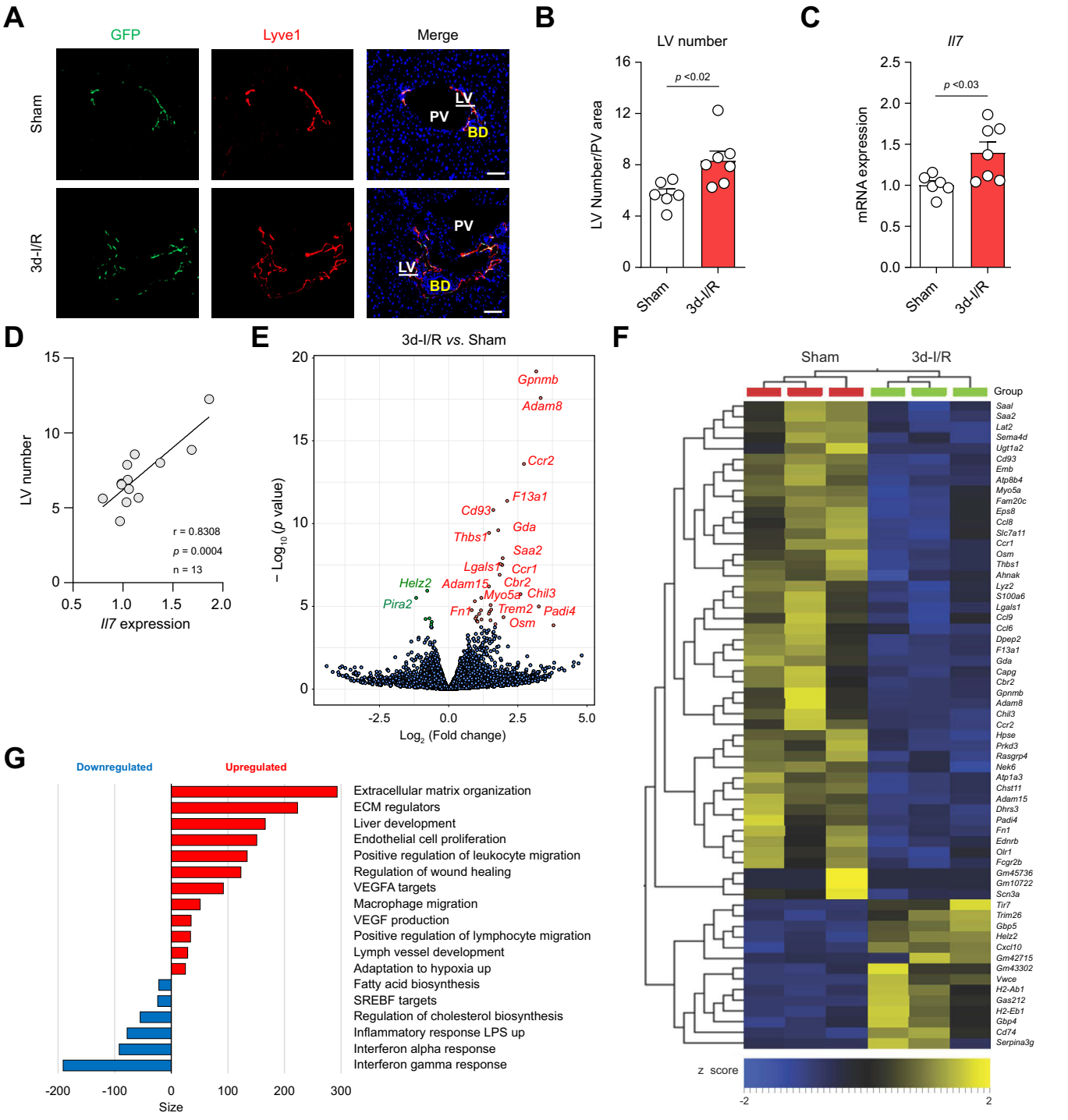

Fig. 4. Altered transcriptomes in LyECs caused by liver ischemia/reperfusion injury. (A–G) I/R surgery was performed on *IL7*$^{GFP/+}$ knock-in mice. Liver tissues were collected from mice 3 days after I/R surgery (3d-I/R, n = 7) or sham surgery (n = 6). (A) GFP (IL7-GFP) and Lyve1 (a marker of lymphatic vessels) immunolabeling in mouse livers from the sham and 3d-I/R groups. Scale bar: 50 μm. (B) Quantification of LV numbers per portal area based on co-labeling of GFP and Lyve1. Data are the mean ± SEM. p = 0.0135 (two-tailed unpaired t test). (C) IL7 expression levels in the livers from sham and 3d-I/R mice. Data are the mean ± SEM. p = 0.0210 (two-tailed unpaired t test). (D) Correlation between liver IL7 expression levels and LV numbers. Two-tailed linear correlation with Pearson correlation coefficients used (E–G) GFP+ cells from PV tree cell fractions isolated from sham and 3d-I/R mice. RNA-seq analysis was performed on isolated GFP+ cells (n = 3 per group). (E) A volcano plot of differentially expressed genes (DEGs) between the 3d-I/R and sham groups. Red: upregulated genes; green: downregulated genes. (F) A heatmap showing DEGs caused by 3d-I/R. (G) Gene Set Enrichment Analysis (GSEA) was conducted to examine functional changes caused by I/R injury. BD, bile duct; GFP, green fluorescent protein; I/R, ischemia/reperfusion; LSECs, liver sinusoidal endothelial cells; LyECs, lymphatic endothelial cells; LV, lymphatic vessel, PV, portal vein; PV tree, portal venous biliary tree.

unique cell surface structure of LyECs, distinct from that of LSECs, is an important area to be explored in the future. Although IL7 has been successfully used as a marker to isolate LyECs from normal livers and livers with I/R injury, further validation is required to determine whether IL7 can also serve as a marker for chronic liver diseases or liver cancer.

Abbreviations

AoEC, aortic endothelial cell; DEGs, differentially expressed genes; EC, endothelial cell; ECM, extracellular matrix; FACS, fluorescence-activated cell sorting; GEO, Gene Expression Omnibus; GFP, green fluorescent protein; GSEA, gene set enrichment analysis; HUVEC, human umbilical venous endothelial cell; IL7, interleukin 7; ILC, innate lymphoid cell; I/R, ischemia/reperfusion; LSEC, liver sinusoidal endothelial cell; LV, lymphatic vessel; LyECs, lymphatic endothelial cells; LYVE1, hyaluronan receptor 1; MP, macrophages, mononuclear phagocytes; pDC, plasmacytoid dendritic cell; PDPN, podoplanin; PROX1, prospero homeobox protein 1; PV tree, portal venous biliary tree; scRNA-seq, single-cell RNA sequencing; SEM, scanning electron microscopy, standard error of mean; UMAP, Uniform Manifold Approximation and Projection; UMI, Unique molecular identifier; VEGF-C, vascular endothelial growth factor-C; VEGF-D, vascular endothelial growth factor-D; VEGFR3, vascular endothelial growth factor receptor 3.

Financial support

We thank the Yale Liver Center for the resources (5P30DK034989-37). This work was funded by NIH grants (R56DK121511, R01DK121511, 1R01DK117597, and 1R21AA031400-01) to YI; (K08AA029182) to MJM.

Conflict of interest

The authors declare no competing interests.

Please refer to the accompanying ICMJE disclosure forms for further details.

Authors' contributions

Conceptualized the research: YY, YI. Designed the methodology: YY, JJ, MG, XL, TU. Performed experiments: YY, JJ, TS, SL, PZ, MG, XL, TU. Analyzed data: YY, RG-M. Visualized the data: YY, RG-M. Designed the graphic: JJ. Wrote the manuscript: YY, JJ. Edited the manuscript: MJM, TU, JP. Provided resources: JP, YI. Provided supervision, YI. Acquired funding, YI. Contributed to and approved this manuscript: all authors.

Data availability statement

The raw data that support the findings of this study have been submitted to NCBI's Sequence Read Archive (SRA) database with the accession number PRJNA1066846. The processed data have been submitted to GEO and will be available upon acceptance of the manuscript.

Acknowledgements

We thank Ms Kathy Harry (Yale Liver Center) for liver cell isolation and Dr Dejian Zhao for bioinformatics analysis. Research reported in this publication used Yale Center for Genome Analysis for RNA sequencing, which was supported by the National Institute of General Medical Sciences of the National Institutes of Health (1S10OD030363-01A1).

Supplementary data

Supplementary data to this article can be found online at https://doi.org/10.1016/j.jhepr.2024.101069.

References

Author names in bold designate shared co-first authorship

[1] Alitalo K. The lymphatic vasculature in disease. Nat Med 2011;17:1371–1380.
[2] Alitalo K, Carmeliet P. Molecular mechanisms of lymphangiogenesis in health and disease. Cancer Cell 2002;1:219–227.
[3] **Jeong J**, **Tanaka M**, Iwakiri Y. Hepatic lymphatic vascular system in health and disease. J Hepatol 2022;77:206–218.
[4] Tanaka M, Iwakiri Y. The hepatic lymphatic vascular system: structure, function, markers, and lymphangiogenesis. Cell Mol Gastroenterol Hepatol 2016;2:733–749.
[5] Tanaka M, Iwakiri Y. Lymphatics in the liver. Curr Opin Immunol 2018;53:137–142.
[6] Burchill MA, Goldberg AR, Tamburini BAJ. Emerging roles for lymphatics in chronic liver disease. Front Physiol 2019;10:1579.
[7] Lukacs-Kornek V. The role of lymphatic endothelial cells in liver injury and tumor development. Front Immunol 2016;7:548.
[8] Su T, Yang Y, Lai S, et al. Single-cell transcriptomics reveals zone-specific alterations of liver sinusoidal endothelial cells in cirrhosis. Cel Mol Gastroenterol Hepatol 2021;11:1139–1161.
[9] Banerji S, Ni J, Wang SX, et al. LYVE-1, a new homologue of the CD44 glycoprotein, is a lymph-specific receptor for hyaluronan. J Cel Biol 1999;144:789–801.
[10] Prevo R, Banerji S, Ferguson DJ, et al. Mouse LYVE-1 is an endocytic receptor for hyaluronan in lymphatic endothelium. J Biol Chem 2001;276:19420–19430.
[11] Joukov V, Pajusola K, Kaipainen A, et al. A novel vascular endothelial growth factor, VEGF-C, is a ligand for the Flt4 (VEGFR-3) and KDR (VEGFR-2) receptor tyrosine kinases. EMBO J 1996;15:290–298.
[12] Breiteneder-Geleff S, Soleiman A, Kowalski H, et al. Angiosarcomas express mixed endothelial phenotypes of blood and lymphatic capillaries: podoplanin as a specific marker for lymphatic endothelium. Am J Pathol 1999;154:385–394.
[13] Wigle JT, Harvey N, Detmar M, et al. An essential role for Prox1 in the induction of the lymphatic endothelial cell phenotype. EMBO J 2002;21:1505–1513.
[14] Ramachandran P, Dobie R, Wilson-Kanamori JR, et al. Resolving the fibrotic niche of human liver cirrhosis at single-cell level. Nature 2019;575:512–518.
[15] Mackall CL, Fry TJ, Gress RE. Harnessing the biology of IL-7 for therapeutic application. Nat Rev Immunol 2011;11:330–342.
[16] Mazzucchelli RI, Warming S, Lawrence SM, et al. Visualization and identification of IL-7 producing cells in reporter mice. PLoS One 2009;4:e7637.
[17] Hara T, Shitara S, Imai K, et al. Identification of IL-7-producing cells in primary and secondary lymphoid organs using IL-7-GFP knock-in mice. J Immunol 2012;189:1577–1584.
[18] Miller CN, Hartigan-O'Connor DJ, Lee MS, et al. IL-7 production in murine lymphatic endothelial cells and induction in the setting of peripheral lymphopenia. Int Immunol 2013;25:471–483.
[19] Jeong J, Tanaka M, Yang Y, et al. An optimized visualization and quantitative protocol for in-depth evaluation of lymphatic vessel architecture in the liver. Am J Physiol Gastrointest Liver Physiol 2023;325:G379–G390.
[20] Sawa Y, Arima Y, Ogura H, et al. Hepatic interleukin-7 expression regulates T cell responses. Immunity 2009;30:447–457.
[21] Alves NL, Richard-Le Goff O, Huntington ND, et al. Characterization of the thymic IL-7 niche in vivo. Proc Natl Acad Sci U S A 2009;106:1512–1517.
[22] Finlon JM, Burchill MA, Tamburini BAJ. Digestion of the murine liver for a flow cytometric analysis of lymphatic endothelial cells. J Vis Exp 2019. https://doi.org/10.3791/58621.
[23] Cogger VC, McNerney GP, Nyunt T, et al. Three-dimensional structured illumination microscopy of liver sinusoidal endothelial cell fenestrations. J Struct Biol 2010;171:382–388.
[24] DeLeve LD, Ito Y, Bethea NW, et al. Embolization by sinusoidal lining cells obstructs the microcirculation in rat sinusoidal obstruction syndrome. Am J Physiol Gastrointest Liver Physiol 2003;284:G1045–G1052.
[25] **Nakamoto S**, **Ito Y**, Nishizawa N, et al. Lymphangiogenesis and accumulation of reparative macrophages contribute to liver repair after hepatic ischemia-reperfusion injury. Angiogenesis 2020;23:395–410.
[26] Kondo Y, Larabee JL, Gao L, et al. L-SIGN is a receptor on liver sinusoidal endothelial cells for SARS-CoV-2 virus. JCI Insight 2021;6:e148999.
[27] Mouta Carreira C, Nasser SM, di Tomaso E, et al. LYVE-1 is not restricted to the lymph vessels: expression in normal liver blood sinusoids and down-regulation in human liver cancer and cirrhosis. Cancer Res 2001;61:8079–8084.
[28] Shetty S, Lalor PF, Adams DH. Liver sinusoidal endothelial cells – gatekeepers of hepatic immunity. Nat Rev Gastroenterol Hepatol 2018;15:555–567.

[29] Liang B, Hara T, Wagatsuma K, et al. Role of hepatocyte-derived IL-7 in maintenance of intrahepatic NKT cells and T cells and development of B cells in fetal liver. J Immunol 2012;189:4444–4450.
[30] Nabekura T, Riggan L, Hildreth AD, et al. Type 1 innate lymphoid cells protect mice from acute liver injury via interferon-γ secretion for upregulating Bcl-xL expression in hepatocytes. Immunity 2020;52:96–108.e109.
[31] Rueschenbaum S, Cai C, Schmidt M, et al. Translation of IRF-1 restricts hepatic interleukin-7 production to types I and II interferons: implications for hepatic immunity. Front Immunol 2020;11:581352.
[32] **Iolyeva M**, **Aebischer D**, Proulx ST, et al. Interleukin-7 is produced by afferent lymphatic vessels and supports lymphatic drainage. Blood 2013;122:2271–2281.